

7 Outer Detector System

7.1 Introduction

In this chapter, we describe the performance and design of the outer detector system for LZ. The principal signal we seek, that of a WIMP scatter depositing 5-50 keV of energy in the central volume of LXe, will never be accompanied by deposited energy in the surrounding detector components. In contrast, the dominant backgrounds that might fake a WIMP signal will deposit energy not only in the central Xe detector but also in the material surrounding it. If we are able to detect these secondary interactions, we can veto the background event. Table 3.8.1.1 shows the major backgrounds in LZ, which include signals from gamma rays with energies in the few-MeV range and neutrons from (α ,n) reactions or created by cosmic-ray interactions.

To reduce these backgrounds to the level required, we surround the large active Xe volume with an integrated detector capable of tagging gamma rays and neutrons with high efficiency. Three detector elements are used to achieve this performance:

- The instrumented “skin” of the Xe, the region outside the LXe TPC (see Chapter 6),
- The gadolinium-loaded liquid scintillator (Gd-LS), and
- The portion of the surrounding water that is instrumented as a muon veto.

The outer detector system comprises the scintillator and water systems. In addition to the performance of the integrated veto system, this chapter describes the design of the outer detector system and modifications needed in the water tank to accommodate the LZ experiment.

7.2 Function and Performance of the Outer Detector

The outer detector serves two critical functions:

1. **To veto neutron and gamma backgrounds with high efficiency.** Although the outer region of the Xe shields the inner region very efficiently, the outer half of the Xe could not be used as part of the fiducial mass without an external veto. By instrumenting the outer skin of the Xe and adding the scintillator veto, we are able to double the fraction of the Xe in which very-low backgrounds are achievable. The outer detector is particularly important for vetoing neutrons, the background that most closely mimics dark-matter scattering.

One risk to the performance of the LZ detector is that some material very close to the Xe could have a concentration of radioactive impurities higher than expected. The combination of the Xe skin and the outer detector serves to mitigate this risk. The integrated veto can suppress most backgrounds even if they are significantly higher than the design goals, with only a slight reduction in fiducial volume.

2. **To help characterize and measure the background.** A claim of a WIMP signal would require extraordinary supporting evidence. The outer detector will provide crucial supporting evidence necessary to establish a discovery. In particular, the only way to measure the neutron background reliably is by measuring the number of low-energy deposit scatters in the TPC that are followed by neutron captures in the outer detector.

The major non-neutrino background sources in LZ are neutrons and gammas from components within the cryostat and beta decays from radon and krypton distributed throughout the Xe. The levels for radon and krypton are designed to be low enough that the activity from both sources combined will be only 20% of that expected from astrophysical neutrinos (see Table 3.8.1.1). The principal goal of the integrated veto system is to reduce the effect of neutron and gamma backgrounds to a level smaller than that caused by radon and krypton over a very large fraction of the active Xe.

Neutrons represent a particularly troublesome background in the absence of an external veto. A neutron scatter produces a nuclear recoil (NR), as does a WIMP scatter, and after scattering they can escape the TPC and skin more easily than a gamma. The neutron background, which is principally produced in (α, n) reactions in materials near the Xe, is more difficult to predict than the gamma background. If a possible WIMP signal is seen, the outer detector will be needed to identify and measure the neutron background with good systematic error. The design requirement for NR background is to limit the background to less than 0.1 count in the 5,600 tonne-day exposure. Without the outer detector, the neutron background in a 5.6-tonne fiducial volume is a few events, so meeting the target requires a veto efficiency of greater than 90% for neutrons escaping the TPC.

The principal sources of gamma background are components in direct contact with the Xe volume, such as the PMTs, the PTFE reflectors, and the titanium inner vessel. Gammas in the few-MeV range can scatter at small angles in the outer region of the TPC, depositing 0.5-10 keV of energy, and then exit the TPC without a second scatter. The primary LZ requirement is that the number of electron recoil (ER) events in the 5,600 tonne-day exposure is less than 27. Meeting this requirement requires a veto efficiency of $>70\%$ for such gammas.

We have carried out simulations to characterize the impact of the outer detector on the background characteristics of the detector. The simulation package used for this work is the same as the one used in LUX, one that is known to reproduce the measured background in LUX very accurately — see also Chapter 4. The results of these simulations are captured in Figure 7.2.1, which shows the spatial distribution of all major radioactive backgrounds that scatter once in the Xe volume.

The left panel of Figure 7.2.1 shows the distribution of single scatters from backgrounds in the Xe TPC. The background in this plot is the sum of the NR background from neutrons, the ER background from gammas, and a uniform source of ER scatters from pp solar neutrinos. The plot assumes S2/S1 cuts that produce a 99.5% rejection of ER backgrounds with acceptance of 50% for NR backgrounds. The figures plot depth (Z) versus radius-squared, so that the area on the plot is proportional to the volume of Xe. The central region is, as expected, extraordinarily free of background. But the background is much higher, within 20 cm of the outer structures, and this is from neutrons and gammas. The white line indicates the fiducial volume, defined as the region in which the background satisfies the design goals for ER and NR

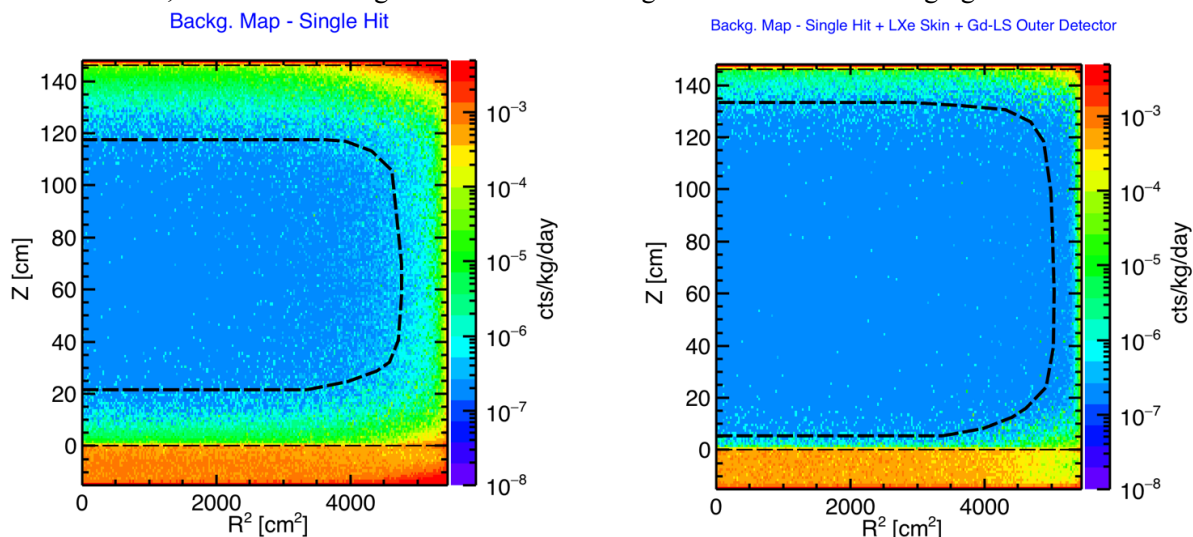


Figure 7.2.1. Total NR background plus ER leakage from sources external to the LXe in the TPC. A discrimination efficiency of 99.5% is applied to ERs from gamma rays and solar pp neutrinos. Left: All single scatters in the TPC. Right: Single scatters in the TPC, vetoing on signals in the instrumented Xe skin and LS detector. Approximate fiducial masses, denoted by the black boundary line, are 3.8 and 5.6 tonnes for the two cases. These plots are taken from Figure 3.8.5.1, which also contains the cases with only LXe skin veto and only Gd-LS veto.

background limits defined above. Without using information from the Xe skin or the outer detector, the fiducial mass is 3.3 tonnes, or about 45% of the active Xe. Most of the active Xe in this case is used as a veto rather than as target material for WIMPs. If one of the component materials in the cryostat were to have a larger amount of radioactivity than the design target, even less of the active Xe would be in the fiducial volume.

The right panel of Figure 7.2.1 shows the performance when vetoing events that also deposit energy in either the instrumented Xe skin or the outer detector. These two systems operate as an integrated high-efficiency veto for neutrons and gammas. The white line shows that the fiducial volume can be extended to within a few centimeters of the edge of the active Xe. The fiducial volume with the integrated veto system is 5.6 tonnes, 1.7 times as large as for a stand-alone Xe TPC. Even if the neutron and gamma backgrounds were significantly higher than assumed in this study, the very-low background needed for effective operation of LZ could be maintained by reducing this fiducial volume by only a small amount.

Because of the large surface area of the LXe vessel, the fiducial volume increases by about 270 kg for every additional centimeter thickness of Xe at the boundary. To meet the LZ background requirements over a 5.6-tonne fiducial volume without using an external veto would require a TPC containing 11 tonnes, 4 tonnes more than the LZ design value.

7.3 Overview of the Outer Detector System

The proposed layout of the LZ outer detector is shown in Figure 7.3.1. A hermetic detector is built from nine vessels fabricated from UVT acrylic. The use of segmented vessels allows fabrication to take place at the manufacturer's facility at considerable cost savings. The sizes of the vessels are chosen to allow straightforward insertion into the water tank and assembly of the full detector inside the water tank. Structural finite element analyses (FEAs) of the vessels have been performed to validate the design without introducing more inert material than is needed for safe operation. The acrylic for the side vessels is 1 inch thick; for the top and bottom vessels, the acrylic is 0.5 inch thick except for the top wall of the top vessel and the bottom wall of the bottom vessel.

The vessels will be viewed by 120 8-inch Hamamatsu R5912 PMTs. The PMTs are mounted on stainless steel frames in the water tank, separated from the Gd-LS vessels by 80 cm. This arrangement gives a light-collection efficiency of about 7% averaged over the volume of the outer detector, corresponding to a light yield of about 130 photoelectrons for a 1-MeV energy deposit. The water shields the Gd-LS from gammas that originate in the R5912 tubes. A low-density water displacer will be used to fill in the gaps between the cryostat and the acrylic vessels and the gaps around the penetrations, to reduce the probability of absorption in inert material. A white diffuse reflector will be placed inside the outer detector vessels to improve collection of the scintillation light.

Simulation of the veto performance showed that the veto efficiency varies slowly with the thickness of the scintillator in the outer detector over the range 50 to 80 cm. This thickness is therefore optimized to reduce the risk of problems during fabrication and assembly. To insert the side vessels into the water tank easily, the scintillator thickness needs to be significantly less than 70 cm. Cleaning the vessels during fabrication requires that the thickness be no less than 61 cm, however, so we chose 61 cm for that thickness.

The liquid scintillator is based upon linear-alkylbenzene (LAB), a hydrocarbon chain with one benzene ring attached. LAB has a flashpoint that exceeds that of diesel fuel, and the safety aspects of diesel fuel in an underground facility have been explored and defined. The LAB is loaded with Gd, 0.1% by mass, via an organic chelating agent, trimethyl hexanoic acid (TMHA). This scintillator mix with 0.1% Gd doping was used by Chooz [1], Palo Verde [2], and Daya Bay [3]. The specific approach adopted by LZ is very similar to that used in the Daya Bay neutrino experiment, but with additional purification to achieve a lower uranium/thorium (U/Th) background.

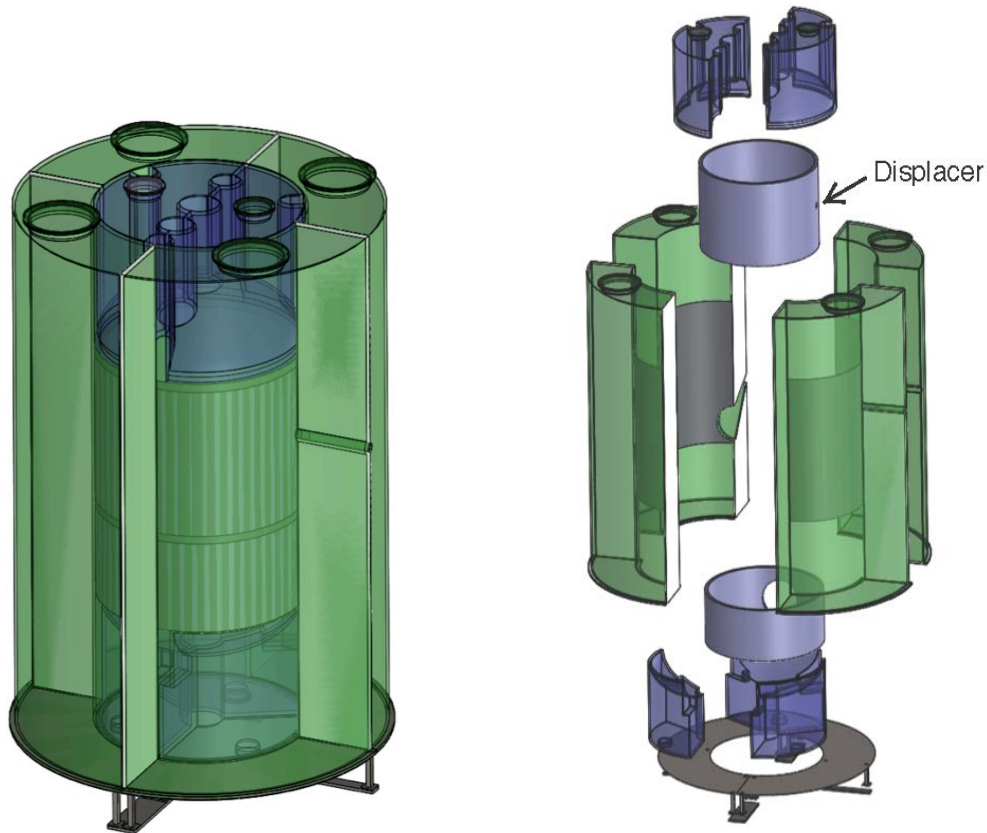


Figure 7.3.1. Layout of the LZ outer detector system, which consists of nine acrylic tanks. The largest are the four quarter-tanks on the sides. Two tanks cover the top, and three the bottom. The exploded view on the right shows the displacer cylinders placed between the acrylic vessels and the cryostat.

Gadolinium is added to the scintillator to increase the efficiency for tagging neutrons while maintaining low veto deadtime. The benefit of using Gd and scintillator for this purpose was demonstrated in the ZEPLIN series of experiments. Neutrons moderated to thermal energies in the scintillator are captured 90% on ^{157}Gd or ^{155}Gd , releasing 3-4 gammas with total energy of 7.9 MeV (^{157}Gd) or 8.5 MeV (^{159}Gd); the remaining 10% of the neutrons are captured on hydrogen, producing a single 2.2-MeV gamma. The Gd captures are tagged with higher efficiency because of the multiple gammas produced and the high energy of those gammas. The Gd reduces the neutron capture time to about 30 μs , compared with about 200 μs in scintillator without Gd. Figure 7.3.2 shows the simulated

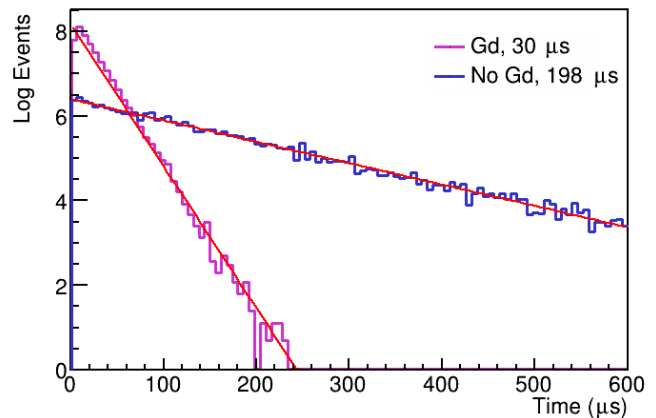


Figure 7.3.2. The simulated distribution of capture times for thermal neutrons in the outer detector for LS with and without Gd.

capture time for low-energy neutrons entering the outer detector. To maintain low deadtime for the veto system requires maintaining excellent radiopurity of the liquid scintillator, even with a veto window of 125 μs that is matched to the capture time with Gd. Without Gd, the veto window would be close to 1 ms, and the radiopurity requirements for the scintillator would be very difficult to meet.

7.4 Mechanical Design and Systems

The 20.8 tonnes of scintillator liquid are contained in nine acrylic vessels, as shown in Figure 7.3.1: four tall vessels on the sides, two vessels that form a plug on the top, and three vessels that form a plug at the bottom. Taken together, the LS system forms a 61-cm-thick detector surrounding the Xe vessel, with several penetrations for connections to the Xe detector and for calibration systems. Similar acrylic vessels were used for the Daya Bay Antineutrino Detectors [3].

The masses and volumes of the nine vessels are shown in Table 7.4.1. The side vessels represent the largest part of the veto mass, holding about 88% of the scintillator. Each of the four side vessels is 427 cm high, extends in radius from 100.3 to 161.3 cm, and covers one-quarter of the full azimuth. A vessel is supported and anchored to a stainless steel base frame, which is in turn anchored to a base plate installed on the floor of the water tank. The net upward force on each side vessel when filled is 5826 N.

The two top vessels form a 61-cm-thick plug that fits inside the side vessels. They will be anchored from the top of the outer cryostat vessel. The three bottom vessels form a plug of the same thickness at the bottom. The penetrations for services and calibrations are positioned within the gaps between the acrylic vessel and in cutouts in the acrylic vessels.

The scintillation light is viewed by PMTs in the surrounding water, so the acrylic used to construct the vessels is chosen to be transparent to photons with wavelengths greater than about 300 nm. The vessels will be filled with LS at the same time that the water tank is filled with water, minimizing the differential pressure on the vessel walls and the stresses on them. This makes it possible to engineer the vessels with acrylic 2.54 cm thick.

The flanges on the detector cryostat protrude about 2 inches outside the cylindrical surface. To avoid building recesses in the acrylic vessels to accommodate these protrusions, a low-density foam will be installed as a water displacer around the outer vessel of the cryostat. This maintains low absorption of gammas between the scintillator and the Xe skin detector.

The vessels will be cleaned inside and leak-checked at the fabrication vendor. They will be wrapped in protective sheets at that time, and placed in double bags before being crated for shipping. The protective sheets will be removed after they are installed in the water tank. The final cleaning of the outside of the vessel will be done at that time.

As a feasibility study, a mock side vessel was slung under the Yates cage, taken down the shaft, and transported to the cart-wash area just outside the LUX experimental hall. We have studied the process of installing the acrylic vessels into the LUX/LZ water tank using a detailed computer model. The acrylic vessel will be transported in a horizontal position to the deck immediately above the water tank. The vessel will then be rotated using lifting eyes at the top and bottom. Figure 7.4.1 demonstrates one step of this process, near the point that requires maximum clearance above the deck. The vessel is lowered in vertical position into the water tank and then transported radially outward to near the wall of the tank. Figure 7.4.2 shows the assembly step at which all of the quadrant vessels are in the tank, and the first one is being brought into place around the cryostat. A white diffuse reflector, Tyvek, is placed at the inner surface of the scintillator vessels, the surface facing the cryostat.

Table 7.4.1. The mechanical characteristics of the nine scintillator vessels.

	Acrylic Volume (m ³)	Acrylic Mass (kg)	LAB Volume (m ³)	LAB Mass (kg)
Side Tank (each)	0.643	759	5.172	4462
Top Tank (each)	0.214	253	0.862	744
Bottom Tank (each)	0.132	156	0.561	484
Total	3.396	4007	24.095	20789

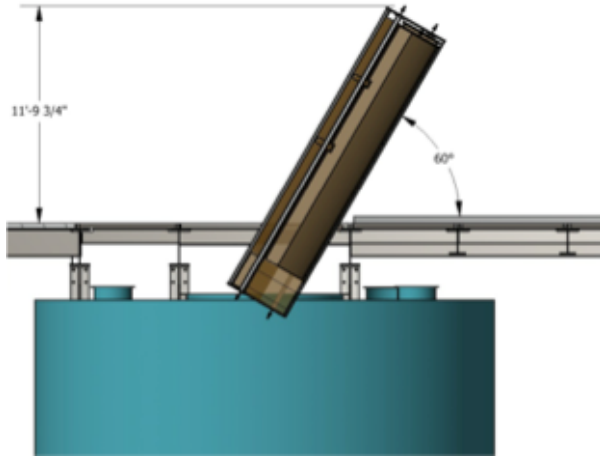


Figure 7.4.1. A step in the assembly sequence for the outer detector system. This shows one of the quadrant vessels at 60°, the point of maximum height above the water tank.

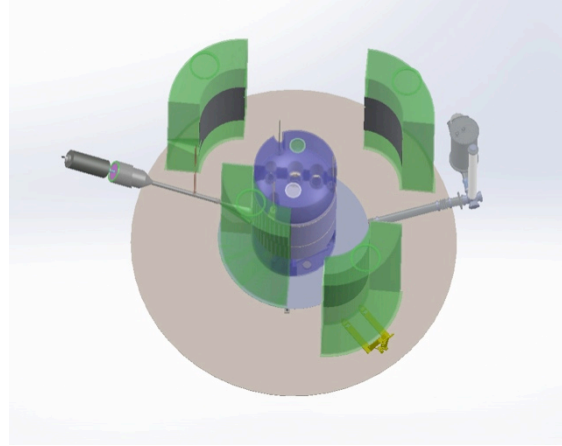


Figure 7.4.2. Another step in the assembly sequence for the outer detector system. This shows the four quadrant vessels in the tank, with one already moved into place around the cryostat.

Preliminary quotations for fabrication of the vessels have been obtained from vendors experienced with previous acrylic vessel fabrication for high-energy physics experiments. A site visit to one of the vendors to discuss design and fabrication has been completed.

7.5 Technical Description of the Liquid Scintillator

We chose Gd-LS for the detection medium to achieve excellent efficiency for neutrons and gammas. Various organic liquid scintillators have been used for neutron tagging due to their production of relatively large numbers of photons at low energies of a few MeV. The neutron-capture reaction occurs on the hydrogen in the organic scintillator, $n + p \rightarrow d + \gamma$, but the cross section is small at 0.332 barns, with a neutron-capture time of about 200 μs . The 2.2 MeV γ -ray is in the energy range of natural radioactivity, which extends to 2.6 MeV.

Gadolinium-loaded scintillators have been used in several experiments designed to measure inverse beta decay from reactor antineutrinos, including Palo Verde, RENO, and Daya Bay. There are several compelling advantages of adding Gd to the scintillator:

- The (n,γ) cross section for natural Gd is very high, 49 kilobarns, with major contributions from ^{155}Gd and ^{157}Gd isotopes. Because of this high cross section, only a small concentration of Gd, 0.1% by mass, is needed in the LS.
- The neutron-capture reaction on Gd releases 8 MeV of energy in a cascade of 3-4 γ rays. The efficiency for detecting at least one of these gammas is very high.
- The time delay for the neutron-capture is also significantly shortened to 30 μs in 0.1% Gd as compared with 200 μs in undoped scintillator. This shortened delay time reduces the accidental background rate by a factor of 7.

To detect the low-neutron/gamma backgrounds with high efficiency, the Gd-LS must have the following key properties:

1. Long optical attenuation length, >10 m at 430 nm (the emission spectrum is shown in Figure 7.5.1);
2. High light yield, 9,000 photons/MeV;
3. Ultralow impurity content, mainly of the natural radioactive contaminants, such as U and Th; and
4. Long-term chemical stability, over the lifetime of the experiment.

All of these properties have been achieved on a large scale for the Daya Bay experiment. We are adopting the same formulation and fabrication techniques to take advantage of this proven performance.

It is necessary to avoid any chemical decomposition, hydrolysis, formation of colloids, or polymerization, which over time can lead to development of color, cloudy suspensions, or formation of gels or precipitates in the scintillator, all of which can degrade the scintillator. Recent

successful demonstration of the above-mentioned key items has been done by reactor electron antineutrino experiments using LAB-based, 0.1% Gd-loaded scintillator.

Assessments of the U/Th contaminations in the Daya Bay scintillator show that Daya Bay has already achieved levels nearly acceptable for the LZ experiment. The LZ requirement is based upon limiting gamma rays in the LXe fiducial volume to a rate lower by a factor of 4 than that expected from the PMTs, cryostat, and PTFE. We estimate the U/Th contamination requirements to be <1.7 and <3.2 ppt by mass, respectively. The three most important ingredients — GdCl₃, LAB, and PPO — of the scintillator mixture have already been analyzed for U/Th contamination by the Daya Bay group. The required levels of contamination for each component are summarized in Table 7.5.1. The required level of ²³⁸U is a factor of 12 below that of Daya Bay. In addition, a level of 0.6 ppt of ⁴⁰K is the required, which is a factor of 12 lower than Daya Bay. KamLAND and Borexino reached contamination levels orders of magnitude lower by filtering and stripping the scintillator solvent. We will be able to meet the targets by inserting a second pass of purification into the production process, one step beyond that applied for Daya Bay. Underground sources of carbon must be used for all organics to meet the ¹⁴C, and the scintillator must be kept out of contact with the atmosphere to avoid ⁸⁵Kr.

The principal development of LZ scintillator will be led by the Brookhaven National Laboratory (BNL) group. The level 3 manager there has considerable experience, including supervision of the development

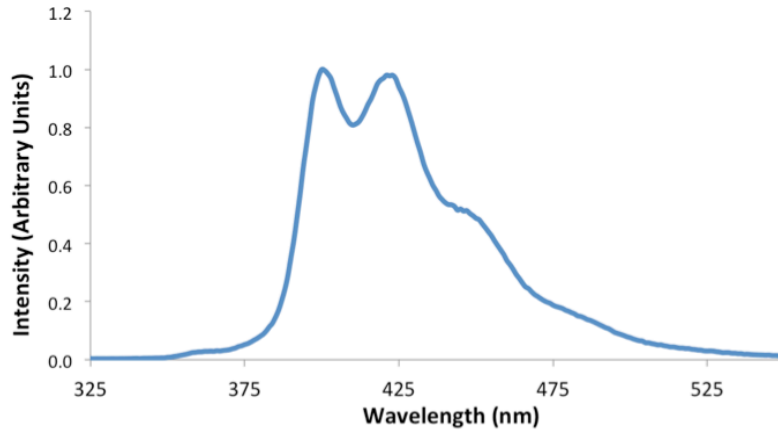


Figure 7.5.1. The emission spectrum of Gd-LS with Gd concentration of 0.2%, based on measurements made of the Daya Bay scintillator.

Table 7.5.1. U/Th impurities in LAB-based Gd-LS. The first column shows required contamination levels for various components of the Gd-LS. Propagation of these contributions to the proposed Gd-LS is summarized in the last two columns.

Part	Raw Values (ppt)				Gram per liter Gd-LS	In 0.1% Gd-LS (ppt)			
	²³⁸ U	²³² Th	⁴⁰ K	¹⁴ C		²³⁸ U	²³² Th	⁴⁰ K	¹⁴ C
LAB	1	0.5	0.4	2.3×10 ⁻⁶	860	1.0	0.5	0.5	2.0×10 ⁻⁶
GdCl ₃	300	1200	20		0.86	0.5	2	0.04	
PPO	20	70	10	50×10 ⁻⁶	3	0.07	0.24	0.04	0.2×10 ⁻⁶
TMHA	20	70	10	50×10 ⁻⁶	3	0.07	0.24	0.04	0.2×10 ⁻⁶
bis-MSB	4000	14000	2000	7×10 ⁻³	0.015	0.07	0.24	0.04	0.2×10 ⁻⁶
Total						1.8	3.4	0.6	3×10⁻⁶
Daya Bay						20	4	7	

and production of the Gd-loaded LS for the Daya Bay experiment. The development of LZ scintillator will be undertaken in two phases: a demonstration phase (to reach ppt levels), followed by a production phase for deployment. The BNL group has a state-of-the-art Liquid Scintillator Development Facility equipped with a variety of instruments (e.g., UV, IR, XRF, LC-MS, medium-scale mixing reactor, thin-film distillatory, 2-m attenuation length system, etc.) for quality assurance that are essential to quality control of the scintillator. The cost-effective plan for the 20.8 tonnes of LZ low-background Gd-LS production will be to carry out the production at the BNL facility and ship the synthesized scintillator to SURF for filling. The scintillator will be produced at a rate of 0.5 tonne per week and will be stored in 55-gallon PTFE-lined drums, which are then shipped to SURF for storage. The purification methods for all components of the Gd-doped scintillator are developed and will be applied to each component before synthesis.

We are building an LS screener, consisting of an acrylic vessel that can hold 30 kg of Gd-LS viewed by three PMTs. We will fill this with scintillator liquid samples from the Gd-LS production line and place it in the LUX water tank, or similar, underground at SURF. By operating in this environment, we will be able to check that the scintillator meets the radiopurity standards.

7.6 Photomultiplier System

Building on the successful use of the Hamamatsu R5912 PMTs in experiments such as MILAGRO, AMANDA, and most recently Daya Bay, the LZ outer detector will use 120 of these same PMTs.

The two existing models for this PMT are R5912 and R5912-02. The latter possesses four more dynode stages and provides higher gain, at the cost of higher dark current and slightly degraded timing characteristics. As LZ does not need the additional gain, the less-expensive model R5912 was chosen. Even for this model, several subcategories exist that represent various quality levels of glass window and photocathode materials. Our assessment of radioactivity levels concluded that the basic model was sufficient for LZ needs and requirements.

The R5912 PMTs are suitable for the outer detector for the following reasons:

1. The spectral response ranges from 300 nm to 650 nm, with a peak wavelength at 420 nm. This matches well the scintillation light from the LAB mix between 390 and 440 nm. The quantum efficiency also covers the relevant range, with an average expected value of ~25% at 430 nm.
2. The PMTs will be submerged in up to 6 m water and must be able to operate in this environment. Daya Bay has been able to demonstrate successful operation of the R5912 assembly at higher pressures than those required for LZ. This experiment used the same assembly that LZ will use.
3. The radioactivity levels of the PMTs and assembly are a fairly weak constraint, thanks to the minimum 80 cm of water that separate them from any active detector volume. Eighty cm of water typically reduces the integrated flux of incoming gammas by more than 2 orders of magnitude, before taking into account geometric effects. For the event rate in the Xe target, the 80 cm of water plus the thickness of the scintillator make the R5912 contribution largely subdominant to internal sources, for both gammas and neutrons. In the scintillator itself, the simulated event rate from PMT radioactivity is 20 Hz (1% downtime would be caused by 125 Hz).

The R5912 PMTs and waterproof assemblies will undergo rigorous individual testing to fully characterize the response and to validate uniform operation and long-term stability for the lifetime of the detector. These tests will include individual electrical behavior, gain measurements, linearity, after-pulsing, dark current, and dark count. In addition, the PMTs will be radioactively screened to make sure the activities are consistent with the values listed in Table 7.6.1.

Table 7.6.1. Additional characteristics of the R5912 PMTs, provided by Hamamatsu.

Characteristic	Value
Number of dynode stages	10
Window material	Borosilicate glass
Photocathode material	Bialkali
Minimum photocathode effective area	284 cm ²
Typical bias voltage for 1e7 gain	1500 V
Maximum voltage	2000 V
Single phe rise time	3.8 ns
Single phe FWHM	2.4 ns
Single phe fall time	55 ns
Typical single phe spectrum peak-to-valley ratio	2.5
Mean QE at 390 nm	25%
Anode linearity at ±2% deviation	20 mA
Pressure rating	0.7 MPa
Radioactivity levels per PMT	²³⁸ U: 900 mBq, ²³² Th: 470 mBq, ⁴⁰ K: 3 Bq

7.7 Water PMT Support System and Optical Calibration System

The LAB scintillation light is viewed by 120 8-inch PMTs in a cylindrical array of 20 ladders with six PMTs each. Figure 7.7.1 shows the plan view of the water-support system. The PMT faces are positioned 70 cm from the outer-detector tank wall. The water between the PMTs and the scintillator vessel shields the active detector elements from radioactivity in the PMT assemblies. In this location, the PMTs also see the Cherenkov light from cosmic-ray muons passing through the water.

The PMT ladders are supported from a circular track mounted on the top of the water tank, with a diameter of 18.5 ft. Attachment points on the tank floor keep them located properly.

The PMT frame is modified slightly from the Daya Bay version. Each PMT has a Finemet magnetic shield to isolate the performance from the local magnetic field. The PMT cables run directly from the PMTs through one of the ports in the top of the water tank to an electronics rack outside. Strain relief is applied at the port and on the ladders.

An optical calibration system will be used to monitor the performance of the outer detector and to maintain calibration. The light will be emitted from 30 LED-driven fibers mounted on the PMT support system, one placed at the center of four PMTs. Small diffusive reflectors will reflect some of the light back to the PMTs. In addition, the Tyvek reflectors inside the side vessels will also reflect light to the PMTs. This system will make it possible to cross-calibrate the responses of the water PMTs and to maintain that calibration over the life of the experiment. In addition, the calibration system will be used to

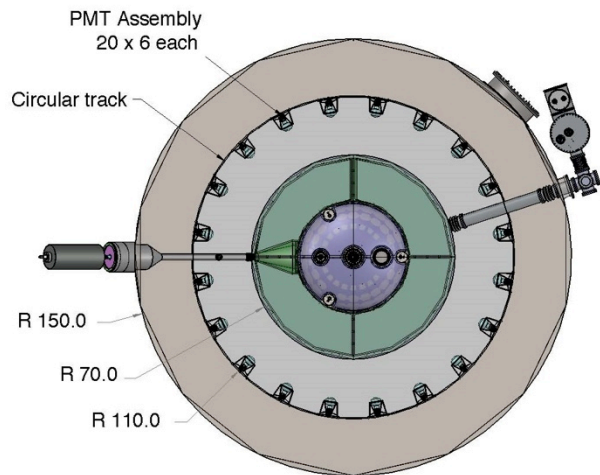


Figure 7.7.1. Plan view of the water PMT support system. The 20 PMT ladders are mounted to a circular track on the roof of the water tank.

check the optical properties of the water and of the scintillator. A prototype of the LED driver for the optical calibration system has already been built and tested. The pulse is less than 2 ns wide, so the width of the observed pulse will be limited by the PMT characteristics.

Fibers will also be installed at the bottom of the side tanks. These will be used to measure the light-attenuation properties of the LS over time. According to simulation, the number of photoelectrons observed per thousand photons produced in the scintillator varies from 4.2 with an absorption length of 9 m to 5.6 with an absorption length of 15 m.

7.8 Scintillator Distribution System and the Filling Process

Each of the nine scintillator vessels has one input and one output line. The side vessels have an input port in the top and an output port in the bottom. The bottom vessels have both ports in the bottom. The top vessels have both ports in the top, with an internal line to the bottom for emptying. The lines are Teflon[®] tubing, with strain relief to the PMT ladders. All 18 lines terminate at a feedthrough panel in the 2-foot flange on the north side of the lid to the water tank. To reduce pressure on the acrylic tanks, a 100-gallon reservoir will be suspended from the floor beams above and next to the north flange of the water tank. The LS will be taken underground in 55-gallon drums. Secondary containment will be provided for all of the lines carrying scintillator. The gas volume above the reservoir will be kept filled with dry nitrogen to minimize the amount of radon entering the liquid. In addition, the vessels will be purged with nitrogen before filling.

To reduce the differential pressure inside and outside the vessels, they will be co-filled with the water tank that encloses them. The hydrostatic pressure on the outer surface of the side vessels varies during the filling process from 1 to 7.8 psi, while the pressure on the inside from the scintillator varies from 1.7 to 7.6 psi. The 100-gallon reservoir is connected to the side tank and filled to match the internal pressure to the outside pressure. Table 7.4.1 shows the net buoyant force on the various tanks when they are filled with scintillator and the surrounding water is in place.

We carried out an FEA of the side vessels during filling to model the stresses on the acrylic during the fill process. The optimal process is to maintain the level of the water outside the vessels to between 10 and 20 inches below the level of the scintillator inside. The FEA shows the maximum tensile stress is 420 psi, occurring when the vessel is about half-full. The design requirement is to keep that stress below 750 psi to avoid crazing. The maximum stress in the long term after filling is 250 psi.

7.9 Threshold, Background Rate, and Deadtime

As described above, a neutron capture in the Gd-LS releases either a few gammas of total energy 8 MeV or a single gamma of energy 2.2 MeV. The neutron-detection efficiency is therefore quite high with the 100 keV threshold planned for the outer detector, which corresponds to about 13 photoelectrons observed. Figure 7.9.1 shows the simulated inefficiency for vetoing 1-MeV background neutrons as a function of threshold in keV. These simulations indicate that the efficiency of the combined veto for neutrons escaping the Xe TPC is about 96%, and the veto efficiency for 1-MeV

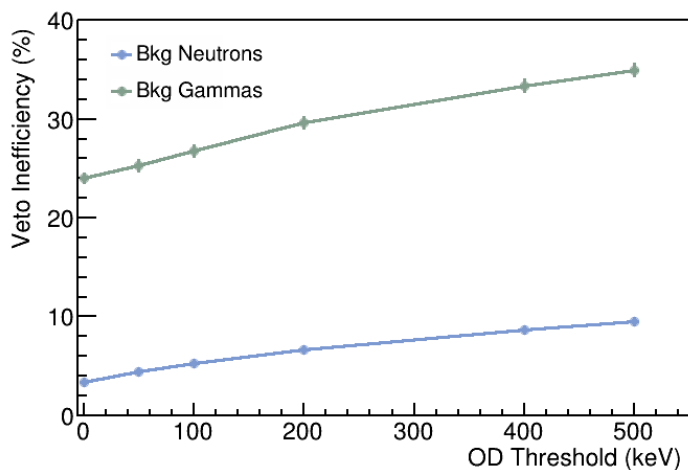


Figure 7.9.1. The simulated inefficiency for vetoing background 1-MeV neutrons and 1-MeV gammas as a function of threshold for the outer detector.

gammas is about 73%. The inefficiency for gammas is dominated by Compton scattering in the inert material, especially the inner wall of the acrylic, and is fairly insensitive to the threshold.

We will read out the outer-detector PMTs each time the Xe TPC produces a trigger, without need of a hardware threshold. We will therefore be able to apply the veto offline, with parameters carefully selected to optimize the veto efficiency. We will apply a neutron veto over a time window of 125 μs with a threshold of no more than 200 keV. In addition, we will apply a gamma veto over a much tighter time window of 1 μs with a threshold of 100 keV. We will set up an outer-detector hardware trigger to calibrate and monitor the background environment.

The sensitivity of the outer detector is estimated to be about 130 photoelectrons/MeV from simulation of LZ and this agrees with benchmarks against similar detectors. Thus, a 100-keV threshold corresponds to about 13 photoelectrons, and the trigger rate will be dominated by alphas, gammas, and betas from the U and Th chains.

Because the time of the low-energy scatter in Xe is determined well by measuring the prompt S1 light, the neutron veto window will be determined by the capture time for neutrons. We presently assume a 125- μs veto window, which is >4 capture lifetimes. To be conservative, we set a goal of keeping the deadtime for this time window at around 2%. This requires keeping the background rate in the outer detector below 160 Hz, which can be met by the radiopurity targets in Table 7.5.1. The width of the veto window needed for high-efficiency neutron vetoing will be determined by studying it with neutron-calibration data.

7.10 Environment, Safety, and Health Issues

The most important safety issue to consider underground is flammability. The flashpoint for LAB is 120-140 $^{\circ}\text{C}$, which makes it a Class IIIB liquid, the lowest hazard category. A Class IIIB liquid is a combustible liquid with a flashpoint at or above 200 $^{\circ}\text{F}$ (93.4 $^{\circ}\text{C}$). OSHA flammable and combustible liquid regulations do not apply to IIIB liquids. The boiling point is greater than 250 $^{\circ}\text{C}$, and the melting point is below -70 $^{\circ}\text{C}$, so it is very stable as a liquid. The density of LAB is 0.86 gm/cm^3 , significantly less than water. In addition, it has very low solubility in water.

The primary risk to consider is a crack in one of the acrylic vessels. The first preventive step is to thoroughly check the integrity of the vessel before introducing the scintillator liquid into it. The second is to monitor the vessel carefully during the filling process. The water tank serves as a secondary containment system for the scintillator. We will install a sensor system into the water-circulation loop that can detect small amounts of LAB. We will also be able to separate LAB from the water in the water treatment. If a significant leak is observed, we will skim the surface of the water to recover most of the scintillator, and then remove the residual scintillator by distillation.

Chapter 7 References

- [1] M. Apollonio *et al.* (CHOOZ), *Eur. Phys. J.* **C27**, 331 (2003), [arXiv:hep-ex/0301017 \[hep-ex\]](#).
- [2] F. Boehm *et al.*, *Phys. Rev. Lett.* **84**, 3764 (2000), [arXiv:hep-ex/9912050 \[hep-ex\]](#); A. G. Piepke, S. W. Moser, and V. M. Novikov, *Nucl. Instrum. Meth.* **A432**, 392 (1999), [arXiv:nucl-ex/9904002 \[nucl-ex\]](#).
- [3] F. P. An *et al.* (Daya Bay), *Nucl. Instrum. Meth.* **A685**, 78 (2012), [arXiv:1202.6181 \[physics.ins-det\]](#); X. Guo *et al.* (Daya Bay), “A Precision measurement of the neutrino mixing angle θ_{13} using reactor antineutrinos at Daya-Bay,” (2007), proposal, [arXiv:hep-ex/0701029 \[hep-ex\]](#).